ARTICLES

Electronic and electromagnetic properties of nanotubes

Gregory Ya. Slepyan and Sergey A. Maksimenko*
Institute of Nuclear Problems, Belarus State University, Bobruiskaya str. 11, Minsk, 220050, Belarus

Akhlesh Lakhtakia†
CATMAS-Computational and Theoretical Materials Sciences Group, Department of Engineering Science and Mechanics, Pennsylvania State University, University Park, Pennsylvania 16802-1401

Oleg M. Yevtushenko‡
Institute of Radiophysics and Electronics, National Academy of Sciences of the Ukraine, Ak. Proskura str. 12, Kharkov, 310085, Ukraine

Anton V. Gusakov*
Institute of Nuclear Problems, Belarus State University, Bobruiskaya str. 11, Minsk, 220050, Belarus
(Received 12 August 1997; revised manuscript received 10 November 1997)

A nanotube is phenomenologically modeled as a chain of atoms wrapped helically on a right circular cylinder. The semiclassical Hamiltonian of an electron is derived, using the Wannier approach for the Schrödinger equation, when the nanotube is exposed to both constant (dc) and high-frequency (ac) electromagnetic fields. The Boltzmann kinetic equation is then solved in the framework of momentum-independent relaxation time approximation. An analytical expression for electric current in a nanotube is derived. The interaction of nonlinearity and chirality is analyzed, chiefly as the dependence of a current chiral angle on the amplitude of the ac electric field. The derived expressions for the electronic transport also help in stating anisotropic impedance boundary conditions on the nanotube surface. Surface wave propagation in a carbon nanotube (CN) is examined. The idea of using CN's as nanowaveguides in the infrared frequency range is established. Convective instability is shown to occur under special conditions in a CN exposed to an axial dc electric field. [S0163-1829(98)03016-1]

I. INTRODUCTION

During the past several years, research on the properties of different fullerenes has proliferated. An extremely attractive feature has emerged: the crystalline structure of a fullerene depends on the conditions of its preparation, with different structures displaying quite different physical response properties. A comprehensive review of the fullerene literature is given by Eletskii and Smirnov in Ref. 1; see also Refs. 2 and 3.

Carbon nanotubes (CN's) are fullerenes with carbon atoms situated regularly on a helical lattice.[4] The base helix of the helical lattice is wrapped along the surface of a cylinder of cross-sectional radius $\sim 10-150$ Å. The wrapping angle, also called the geometric chiral angle (GCA), is usually a few degrees.[5] Having helical symmetry, CN's are quasi-one-dimensional chiral systems,[6,7] on whose mechanical and electronic properties much attention has been lavished.[8]

CN's not only possess very high strength-to-weight ratios,[9] but also have fascinating electromagnetic properties. Recent experimental studies[10] confirmed that a CN can be metallic, semiconducting or even nonmetallic, depending on its tubular radius and GCA. Lou, Nordlander and Smalley,[11] Miyamoto, Louie, and Cohen,[12] Saito, Dresselhaus, and Dresselhaus,[13] and Benedict, Louie, and Cohen[14] examined the response of a CN immersed in an electrostatic field, while Kasumov *et al.*[15] and Langer *et al.*[16] measured the electrical resistance of a CN immersed in a magnetostatic field. A quantum-mechanical treatment of charge-carrier motion in the presence of an external magnetic field was developed by Kibis[17] and Romanov and Kibis.[18] Electron-photon interaction in CN's was theoretically investigated by Romanov,[19] Romanov and Kibis,[20] Chico *et al.*[21] and Langer *et al.*[16]

Along with CN's, nanotubes of graphitic compounds $B_xC_yN_z$, for example, BC_2N, have been produced and extensively studied in recent years.[22–24] According to Ref. 12, such nanotubes are semiconductors independently of their geometry.

Two broad theoretical approaches for electron transport in nanotubes have emerged. The first approach comprises first-principles numerical simulations, as exemplified by Miyamoto, Louie, and Cohen.[12] The other approach requires the creation of phenomenological models that yield somewhat rough but analytically tractable results. As an example, the phenomenological model of a CN as a chain of carbon atoms located on a base helix was investigated by Romanov and colleagues.[17–20]

Miyamoto, Louie, and Cohen[12] computed the current excited in carbon and BC_2N nanotubes immersed in an electro-

static field. Let j_z be the current parallel to the tubular (i.e., the z) axis, and j_c the circumferential current, so that a current chiral angle (CCA),

$$\gamma = \tan^{-1}(j_z/j_c), \tag{1}$$

can be defined. First-principles numerical simulations showed that $\gamma \neq \pi/2$ as well as that the GCA and the CCA are unequal, even though the surface conductivity of the monatomic curved surface of the CN was taken to be isotropic. Kasumov *et al.*[15] and Langer *et al.*[16] measured the resistance of a single CN, their data being in qualitative accord with theoretical results. Most importantly, the two experimental reports established the validity of theoretical models of CN's isolated from one another as well as from any other form of matter.

The conductivity of a nanotube immersed in a high-frequency electromagnetic field in addition to an electrostatic field is of importance for two main reasons. First, exposure to ac electric fields may lead to new techniques for probing carbon microstructures. Second, a nanotube may stand duty as a tool for controlling electromagnetic radiation in specified frequency ranges (for instance, infrared and optical). These issues, apparently not discussed in the literature, constitute the main goals of this paper.

The procedure for describing the electromagnetic response of a nanotube is complicated. It entails finding a self-consistent solution of (i) the equation describing charge-carrier motion, and (ii) the frequency-domain Maxwell equations for electromagnetic fields excited by the charge carriers.

A CN has a two-scale periodicity: one due to the helical pitch (along the z axis), the other from the interatomic distances along the base helix. Also, in a wide variety of real samples, the dynamics of charge carriers in a CN can be described with good accuracy in the framework of the tight-binding approximation. Thus, as a CN is a high-order structure with tight-bound electrons, albeit with an unusual geometry, the methods and standard approximations originally developed for systems of tight-bound electrons, such as quantum superlattices,[25–27] are also applicable after some modification. In particular, the semiclassical approach allows us to decouple the solution of the equation of motion from that of the Maxwell equations, and is well suited for elucidating the electromagnetic response of a single CN. An analogous approach is possible for BC_2N nanotubes.

In this paper we extend a theory outlined recently by us.[28,29] We start from a comprehensive description of electronic properties and transport and then, using the derived transport equations, we pass to the realm of electromagnetics. The outline of the paper is as follows: In Sec. II the phenomenological model of a nanotube is presented. It is used in Sec. III to derive the semiclassical Hamiltonian of an electron on the surface of a nanotube. The electron current induced in a CN exposed to ac and dc electric fields simultaneously is determined in Sec. IV. Electromagnetic jump conditions across the nanotube surface are delineated in Sec. V. These lead in Sec. VI to the dispersion equation of surface electromagnetic waves on a CN, when the electrostatic field is absent. The idea of a CN as a nanowaveguide is proposed. Convective instability is shown in Sec. 7 to occur, under special conditions, in a CN nanowaveguide exposed to an axial dc electric field. Gaussian notation is used in this paper for electromagnetic fields and related quantities.

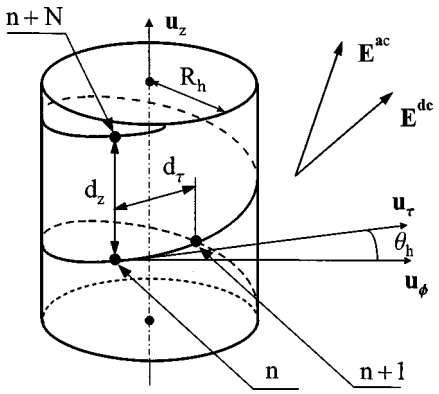

FIG. 1. Schematic of the carbon nanotube geometry. All carbon atoms are numbered consecutively along the base helix.

II. PHENOMENOLOGICAL MODEL OF A NANOTUBE

We start with carbon nanotubes considering an infinitely long chain of carbon atoms wrapped along a base helix as the model of a single CN,[17–20] as shown in Fig. 1. In this phenomenological model, the hexagonal crystalline structure of graphite is reproduced approximately. The chief merit of this model is its analytical tractability, which readily yields physically interpretable results. In addition, the model yields correct qualitative descriptions of various electronic processes, which are corroborated by the first-principles numerical simulations of Miyamoto, Louie, and Cohen.[12]

Let the variable s denote the arc length measured along the base helix from the intersection of the base helix and the plane $z=0$. The position vector of a point on the base helix can be denoted by

$$\mathbf{r}(s) = \frac{\sigma_h^2}{\rho_h}\left\{\cos\left[\frac{z_h(s)}{\sigma_h}\right]\mathbf{u}_x + \sin\left[\frac{z_h(s)}{\sigma_h}\right]\mathbf{u}_y\right\} + z_h(s)\mathbf{u}_z. \tag{2}$$

Here, $z_h(s)$ is the perpendicular distance of that point from the plane $z=0$; $(\mathbf{u}_x, \mathbf{u}_y, \mathbf{u}_z)$ is the triad of cartesian unit vectors; σ_h^{-1} and ρ_h^{-1} are the torsion and curvature of the base helix,[30] respectively; while $R_h = \sigma_h^2/\rho_h$ is the helical radius; $p_h = 2\pi\sigma_h$ is the helical pitch, and $\theta_h = \tan^{-1}(\rho_h/\sigma_h)$ is the GCA.

More convenient than the cartesian coordinate system is Serret-Frenet coordinate system[30] attached to the base helix. The unit Serret-Frenet vectors $(\mathbf{u}_\tau, \mathbf{u}_n, \mathbf{u}_b)$ are related to the unit vectors $(\mathbf{u}_\rho, \mathbf{u}_\phi, \mathbf{u}_z)$ of the cylindrical coordinate system as follows:

$$\mathbf{u}_\tau(s) = \mathbf{u}_\phi(s)\cos\,\theta_h + \mathbf{u}_z\,\sin\,\theta_h,$$

$$\mathbf{u}_n(s) = -\mathbf{u}_\rho(s),$$

$$\mathbf{u}_b(s) = -\mathbf{u}_\phi(s)\sin\,\theta_h + \mathbf{u}_z\,\cos\,\theta_h. \tag{3}$$

Here, $\mathbf{u}_\tau$ is tangential to the base helix described by Eq. (2), while $\mathbf{u}_n$ and $\mathbf{u}_b$ are unit vectors along the normal and the binormal directions, respectively. The unit vectors $\mathbf{u}_\rho(s)$ and $\mathbf{u}_\phi(s)$ carry their dependency on s, as they are the unit cylindrical vectors at a point $\mathbf{r}(s)$ on the base helix. In the sequel, $a_z=\mathbf{a}\cdot\mathbf{u}_z$ and $a_\tau=\mathbf{a}\cdot\mathbf{u}_\tau$, respectively, denote the projections of a vector $\mathbf{a}$ along the tubular axis and the base helix.

A complete turn of the base helix accommodates $N\gg 1$ regularly spaced carbon atoms. The interatomic distances for electronic jumps along the tubular axis and the base helix are, respectively, given by the expressions $d_z=p_h$ and $d_\tau=2\pi\sigma_h/N\sin\theta_h$. We take $N\gg 1$ in this work so that the condition

$$\frac{d_\tau}{R_h}=\frac{2\pi}{N\cos\theta_h}\ll 1 \tag{4}$$

is ensured.

The described framework is *general* because, in addition to chiral CN's, it can accommodate (i) an *achiral carbon nanotube*[31] as a system of coaxially stacked circular atomic chains, and (ii) a BC_2N *nanotube* as comprising two atomic helices wrapped along a cylinder and shifted with respect to one another along the cylinder's axis, with one helix containing carbon atoms and the other formed by alternating nitrogen and boron atoms.

After assuming the tight-binding approximation to be valid, chiral and achiral CN's as well as BC_2N nanotubes can be analyzed in a unified manner, as shown later in this paper.

III. SEMICLASSICAL HAMILTONIAN OF AN ELECTRON IN A NANOTUBE

Let us begin with a CN. Following Okotrub *et al.*,[2] Romanov[18] and Kibis and Romanov,[20] we assume that the behavior of electrons in a CN can be adequately represented by the simplified tight-binding approximation for the lowest conduction band. Thus we assume that the CN is in the semiconducting state.

The phenomenological model of a single CN allows us to apply the Wannier equation,

$$i\hbar\dot{C}_n=E_0C_n-\frac{\Delta_\tau}{2}\{\exp(i\varphi_{n+1})C_{n+1}+\exp(i\varphi_{n-1})C_{n-1}\}-\frac{\Delta_z}{2}\{\exp(i\varphi_{n+N})C_{n+N}+\exp(i\varphi_{n-N})C_{n-N}\}, \tag{5}$$

in the site representation for the amplitudes C_n of the electronic wave function in order to investigate the motion of charge carriers.[20] The following notation is used in Eq. (5): $\dot{C}_n\equiv\partial C_n/\partial t$;

$$\varphi_{n\pm 1}=\frac{e}{\hbar c}\int_{n\pm 1}^{n}A_\tau ds, \tag{6}$$

$$\varphi_{n\pm N}=\frac{e}{\hbar c}\int_{n\pm N}^{n}A_z dz; \tag{7}$$

A_z and A_τ are the components of the vector potential $\mathbf{A}(t)$ of the total externally applied field; e is the electronic charge, c is the light speed in vacuum and $\hbar$ is the Planck constant; E_0 is the energy of an outer-shell electron in an isolated carbon atom; Δ_z and Δ_τ are the real overlapping integrals for jumps along the tubular axis and the base helix, respectively. The last two quantities are phenomenological adjustable parameters to be determined for a real CN by first-principles numerical calculations; their estimates are given in, e.g., Ref. 18.

The second term on the right side of Eq. (5) describes the interaction of an electron with two neighboring sites in the same turn of the helix, while the third describes the interaction of an electron with corresponding sites in the two adjacent turns. Let us introduce shift operators for the two types of interactions as follows:

$$\exp\left\{d_z\frac{\partial}{\partial z}\right\}F(z)=F(z+d_z),$$

$$\exp\left\{d_\tau\frac{\partial}{\partial s}\right\}F(s)=F(s+d_\tau). \tag{8}$$

Furthermore, let us effect the substitutions

$$\frac{\partial}{\partial z}\to -i\frac{\hat{\mathcal{P}}_z}{\hbar},\quad \frac{\partial}{\partial s}\to -i\frac{\hat{\mathcal{P}}_\tau}{\hbar}, \tag{9}$$

with the operators $\hat{\mathcal{P}}_z$ and $\hat{\mathcal{P}}_\tau$ corresponding to the components of the canonical momentum. Assuming that the pitch of the base helix is small compared with the characteristic length scale of the externally applied field, we set

$$\phi_{n+N}\simeq -\varphi_{n-N}. \tag{10}$$

Similarly, assuming that the projections A_τ at any three adjacent sites $n-1$, n, and $n+1$ along the base helix are equal, we also set

$$\phi_{n+1}\simeq -\varphi_{n-1}. \tag{11}$$

The result of the foregoing manipulations is that Eq. (5) simplifies to

$$i\hbar\dot{C}_n=\hat{H}C_n(t), \tag{12}$$

where

$$\hat{H}=E_0-\Delta_z\cos\left(\frac{\hat{\mathcal{P}}_z d_z}{\hbar}+\varphi_{n+N}\right)-\Delta_\tau\cos\left(\frac{\hat{\mathcal{P}}_\tau d_\tau}{\hbar}+\varphi_{n+1}\right) \tag{13}$$

is the Hamiltonian operator.

We remark here that, in general, one jump along the tubular axis and N jumps along the base helix are not equivalent, i.e.,

$$\exp\left\{d_z\frac{\partial}{\partial z}\right\}\neq\exp\left\{Nd_\tau\frac{\partial}{\partial s}\right\}. \tag{14}$$

This is because the electron velocities near the final site differ for the two jumps, although both jumps begin at the same site l (with the same initial velocity) and end at the same site $N+l$ also. The electron velocity has a circumferential com-

ponent for motion along the base helix but not for motion along the tubular axis. This indicates that a CN is a purely quantum structure, and the classical minimum action principle cannot be stated because quantum theory allows different paths connecting a pair of atoms.

Now, from Eq. (13) we are in a position to find expressions for the classical Hamiltonian H of an electron in a CN. According to the correspondence principle, the momentum operator is replaced by the value of the canonical momentum $\mathbf{P}$. In doing so, we consider the z- and the τ- components of the momentum as mutually independent, neglecting the interference between the axial and the helical paths connecting a pair of atoms. This actually means that we do not take transverse motion quantization into account.[32] Previously,[2,18,20] the interference was claimed to be the main mechanism for the chirality of certain physical effects. But in this paper, we focus on another, very different physical mechanism—which is purely classical but, nevertheless, allows chirality to substantially modify electron transport in a CN.

Let the externally applied electric field have both high-frequency (ac) and constant (dc) components:

$$\mathbf{E}(t)=\mathbf{E}_{\rm dc}+\mathbf{E}_{\rm ac}^{(1)}\cos(\omega t)+\mathbf{E}_{\rm ac}^{(2)}\sin(\omega t), \tag{15}$$

where $\mathbf{E}_{\rm dc}$, $\mathbf{E}_{\rm ac}^{(1)}$ and $\mathbf{E}_{\rm ac}^{(2)}$ are time-independent, real-valued vectors. The two harmonic terms on the right side of Eq. (15) allow the incorporation of an arbitrarily polarized electromagnetic field in our treatment. We impose the condition that the electric field varies slowly in space so that we can neglect the effects of spatial nonhomogeneity. The concrete conditions for what *slowly varies* means can be different in different contexts. Clearly, there cannot be appreciable nonhomogeneous effects if the externally applied field is virtually uniform over the entire CN, which condition is assumed in Sec. IV for treating electron transport. But a weaker condition is taken in Sec. VI for surface wave propagation in a CN.

The time-varying vector potential of the applied external field (15) is as follows:

$$\mathbf{A}(t)=-c\mathbf{E}_{\rm dc}t-\frac{c}{\omega}\,\mathbf{E}_{\rm ac}^{(1)}\sin(\omega t)+\frac{c}{\omega}\,\mathbf{E}_{\rm ac}^{(2)}\cos(\omega t). \tag{16}$$

As $\mathbf{E}_{\rm dc}\cdot\mathbf{u}_z$, $\mathbf{E}_{\rm ac}^{(1)}\cdot\mathbf{u}_z$ and $\mathbf{E}_{\rm ac}^{(2)}\cdot\mathbf{u}_z$ are spatially uniform, Eqs. (7) and (16) together yield

$$\varphi_{n+N}=\Omega_z^{\rm dc}t+\xi_{z1}^{\rm ac}\sin(\omega t)-\xi_{z2}^{\rm ac}\cos(\omega t), \tag{17}$$

where

$$\Omega_z^{\rm dc}=\left(\frac{ed_z}{\hbar}\right)\mathbf{E}_{\rm dc}\cdot\mathbf{u}_z, \tag{18}$$

and the ratios

$$\xi_{z1}^{\rm ac}=\left(\frac{ed_z}{\hbar\omega}\right)\mathbf{E}_{\rm ac}^{(1)}\cdot\mathbf{u}_z,\quad \xi_{z2}^{\rm ac}=\left(\frac{ed_z}{\hbar\omega}\right)\mathbf{E}_{\rm ac}^{(2)}\cdot\mathbf{u}_z \tag{19}$$

relate the angular Stark frequencies $[(ed_z/\hbar)\mathbf{E}_{\rm ac}^{(1,2)}\cdot\mathbf{u}_z]$ to the angular frequency ω of the high-frequency field. Consequently, the classical analog of the second term on the right side of Eq. (13) may be written as follows:

$$H_z=-\Delta_z\cos\left[\frac{P_zd_z}{\hbar}+\Omega_z^{\rm dc}t+\xi_{z1}^{\rm ac}\sin(\omega t)-\xi_{z2}^{\rm ac}\cos(\omega t)\right]. \tag{20}$$

Now we come to the classical analog H_τ of the third term on the right side of Eq. (13). In evaluating the right side of Eq. (6), spatial nonhomogeneity is encountered because $\mathbf{u}_\tau(s)$ depends on s. However, using the inequality (4), we quickly get the approximate relation

$$\varphi_{n+1}\approx\Omega_\tau^{\rm dc}t+\xi_{\tau1}^{\rm ac}\sin(\omega t)-\xi_{\tau2}^{\rm ac}\cos(\omega t), \tag{21}$$

where $\Omega_\tau^{\rm dc}$, $\xi_{\tau1}^{\rm ac}$, and $\xi_{\tau2}^{\rm ac}$ are obtained on replacing the subscript z by τ in Eqs. (18) and (19). Thus,

$$H_\tau=-\Delta_\tau\cos\left[\frac{P_\tau d_\tau}{\hbar}+\Omega_\tau^{\rm dc}t+\xi_{\tau1}^{\rm ac}\sin(\omega t)-\xi_{\tau2}^{\rm ac}\cos(\omega t)\right]. \tag{22}$$

The full semiclassical Hamiltonian of an electron in a CN finally emerges from Eqs. (13), (20), and (22) as

$$\begin{aligned}H(P_\tau,P_z,s,t)=E_0-\Delta_z\cos\Bigg[&\frac{P_zd_z}{\hbar}+\Omega_z^{\rm dc}t+\xi_{z1}^{\rm ac}\sin(\omega t)\\&-\xi_{z2}^{\rm ac}\cos(\omega t)\Bigg]-\Delta_\tau\cos\Bigg[\frac{P_\tau d_\tau}{\hbar}+\Omega_\tau^{\rm dc}t\\&+\xi_{\tau1}^{\rm ac}\sin(\omega t)-\xi_{\tau2}^{\rm ac}\cos(\omega t)\Bigg].\end{aligned} \tag{23}$$

This general expression allows us to develop the semiclassical equation of electron motion so that electron transport in CN's can be addressed. The parameters $\Delta_{z,\tau}$ and $d_{z,\tau}$ must be chosen so that the transition from a chiral nanotube to a (monolayer) planar graphite sheet yields isotropic conductivity. Therefore,

$$\Delta_z=\Delta_\tau,\quad d_z=d_\tau \tag{24}$$

must be used in Eq. (23). Furthermore, in view of the relation $\tan\theta_h=d_z/2\pi R_h$, we must take into account that $\theta_h\to0$ when $R_h\to\infty$ for the transition to the planar sheet.

In order to apply Eq. (23) for an achiral CN, it suffices to replace P_τ by P_φ. The semiclassical Hamiltonian of electrons in a BC_2N nanotube can also be written in the form of Eq. (23), after effecting the change $d_{z,\tau}\to2d_{z,\tau}$ together with corresponding adjustment of the overlapping integrals, but the conditions (24) are invalid because BC_2N planar sheets have anisotropic conductivity.

IV. ELECTRONIC CURRENT IN A NANOTUBE

A. Electron fluxes

Let us commence with the Boltzmann kinetic equation,

$$\frac{\partial f(\mathbf{p},t)}{\partial t}+\dot{p}_z\frac{\partial f(\mathbf{p},t)}{\partial p_z}+\dot{p}_\tau\frac{\partial f(\mathbf{p},t)}{\partial p_\tau}=\mathcal{I}(F(\mathbf{p});f(\mathbf{p},t)), \tag{25}$$

for the time-varying distribution function f. Here, F is the equilibrium distribution function, $\mathcal{I}(F;f)$ is the collision integral, and

$$p_z = P_z + \hbar\varphi_{n+N}/d_z, \quad p_\tau = P_\tau + \hbar\varphi_{n+1}/d_\tau \tag{26}$$

are the components of the electron momentum $\mathbf{p}$ with

$$\dot{p}_z = e\mathbf{E}(t)\cdot\mathbf{u}_z, \quad \dot{p}_\tau = e\mathbf{E}(t)\cdot\mathbf{u}_\tau. \tag{27}$$

In accordance with the previous section and Ref. 33, we use the Boltzmann equilibrium distribution function; thus,

$$F(\mathbf{p}) = C\ \exp\left\{\frac{\Delta_z\ \cos(p_z d_z/\hbar) + \Delta_\tau\ \cos(p_\tau d_\tau/\hbar)}{k_B T}\right\}, \tag{28}$$

where

$$C = \frac{d_z d_\tau n_o}{2I_0\left(\dfrac{\Delta_\tau}{k_B T}\right) I_0\left(\dfrac{\Delta_z}{k_B T}\right)}, \tag{29}$$

n_0 is the surface charge density, and $I_0(\cdot)$ is the modified Bessel function of order 0.

The components v_z and v_τ of the electron velocity $\mathbf{v}$ are calculated from Eq. (23) as[33]

$$v_z(p_z) = \frac{\Delta_z d_z}{\hbar}\ \sin\left(\frac{p_z d_z}{\hbar}\right), \quad v_\tau(p_\tau) = \frac{\Delta_\tau d_\tau}{\hbar}\ \sin\left(\frac{p_\tau d_\tau}{\hbar}\right); \tag{30}$$

while the electron fluxes along the tubular axis and the base helix, respectively, are given by

$$\mathcal{Z} = \frac{2e}{(2\pi\hbar)^2}\int\int v_z(p_z) f(\mathbf{p},t)\, dp_\tau dp_z, \tag{31}$$

$$\mathcal{S} = \frac{2e}{(2\pi\hbar)^2}\int\int v_\tau(p_\tau) f(\mathbf{p},t)\, dp_\tau dp_z, \tag{32}$$

where the integrations are carried out over the first Brillouin zone. From these two fluxes, expressions for the axial and the circumferential components of the time-varying current emerge as follows:

$$j_z = \mathcal{Z} + \mathcal{S}\ \sin\ \theta_h, \quad j_c = \mathcal{S}\ \cos\ \theta_h. \tag{33}$$

In view of the inequality (4), we ignore the spatial inhomogeneity arising from $\mathbf{u}_\tau(s)$. Hence, the momentum-independent relaxation time approximation[25] can be invoked so that

$$\mathcal{I}(F(\mathbf{p});f(\mathbf{p},t)) \approx \nu[F(\mathbf{p}) - f(\mathbf{p},t)], \tag{34}$$

where ν is the relaxation frequency. Substituting Eq. (34) on the right side of the kinetic equation (25), and using the method of characteristics,[34] we obtain

$$f(\mathbf{p},t) = F\left(\mathbf{p} + \frac{e}{c}\mathbf{A}(t),0\right)e^{-\nu t} + \nu\int_0^t e^{-\nu t'} F\left\{\mathbf{p} + \frac{e}{c}[\mathbf{A}(t) - \mathbf{A}(t-t')]\right\} dt'. \tag{35}$$

Our interest lies chiefly in evaluating the steady-state current, which means that the condition $\nu t \gg 1$ holds hereafter. Consequently, the first term on the right side of Eq. (35) is negligible and the upper limit t of the integral in the second term can be replaced by ∞. After substituting Eqs. (28) and (35) in Eqs. (31) and (32), the integrations over p_z and p_τ are carried out. The algebraic manipulations are assisted by the formula[35]

$$\exp(\alpha\ \cos\ \theta) = \sum_{m=0}^{\infty}\ (2-\delta_{m0}) I_m(\alpha)\cos(m\theta), \tag{36}$$

where $\delta_{mm'}$ is the Kronecker delta and $I_m(\cdot)$ is the modified Bessel function of order m. Finally, we derive the steady-state electron fluxes,

$$\mathcal{Z} \approx \nu j_z^0 \int_0^\infty \exp(-\nu t')\sin\{\Omega_z^{\rm dc} t' + \xi_{z1}^{\rm ac}[\sin\ \omega t - \sin\ \omega(t - t')] + \xi_{z2}^{\rm ac}[\cos\ \omega t - \cos\ \omega(t-t')]\} dt', \tag{37}$$

$$\mathcal{S} \approx \nu j_\tau^0 \int_0^\infty \exp(-\nu t')\sin\{\Omega_\tau^{\rm dc} t' + \xi_{\tau1}^{\rm ac}[\sin\ \omega t - \sin\ \omega(t - t')] + \xi_{\tau2}^{\rm ac}[\cos\ \omega t - \cos\ \omega(t-t')]\} dt', \tag{38}$$

with

$$j_z^0 = n_0\ \frac{e d_z \Delta_z}{\hbar}\ \frac{I_1(\Delta_z/k_B T)}{I_0(\Delta_z/k_B T)}, \quad j_\tau^0 = n_0\ \frac{e d_\tau \Delta_\tau}{\hbar}\ \frac{I_1(\Delta_\tau/k_B T)}{I_0(\Delta_\tau/k_B T)}. \tag{39}$$

Equations (33) and (37)–(39) are the basic relations describing electron transport in carbon and BC_2N nanotubes. They are used in Secs. 4.2 and 4.3 for investigating electron transport when the nanotube is immersed in the externally applied field (15). In conjunction with the frequency-domain Maxwell equations, they are also useful for elucidating wave propagation phenomena.

B. dc conductivity of a nanotube

Let us consider the special case when the high-frequency components of $\mathbf{E}(t)$ are absent and $\mathbf{E}_{\rm dc} = E_z^{\rm dc}\mathbf{u}_z$. Then, $\xi_{z1,2}^{\rm ac} = \xi_{\tau1,2}^{\rm ac} = 0$ and $E_\tau^{\rm dc} = E_z^{\rm dc}\ \sin\ \theta_h$. Equations (37) and (38) easily yield

$$\mathcal{Z} \approx \frac{j_z^0 \nu \Omega_z^{\rm dc}}{(\Omega_z^{\rm dc})^2 + \nu^2}, \quad \mathcal{S} \approx \frac{j_\tau^0 \nu \Omega_\tau^{\rm dc}}{(\Omega_\tau^{\rm dc})^2 + \nu^2}, \tag{40}$$

so that the dc current components

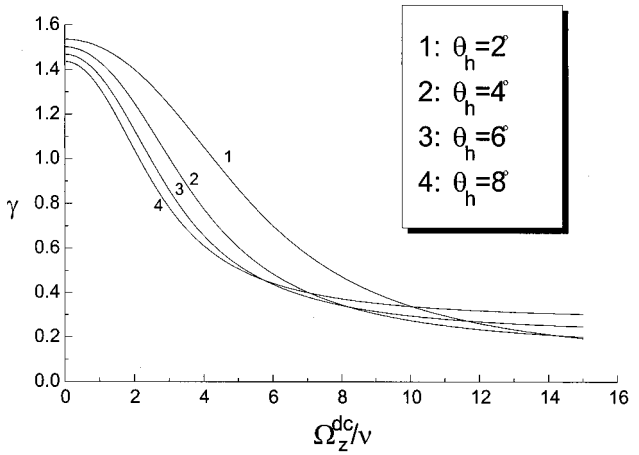

FIG. 2. The dependence of the current chiral angle γ on the amplitude of an axially applied electrostatic field for different geometric chiral angles θ_h; ν is the relaxation frequency, $\Omega_z^{\rm dc}=(ed_z/\hbar)\mathbf{E}_{\rm dc}\cdot\mathbf{u}_z$ and $\mathbf{E}_{\rm ac}=\mathbf{0}$.

$$j_z^{\rm dc}\approx\frac{j_z^0\nu\Omega_z^{\rm dc}}{(\Omega_z^{\rm dc})^2+\nu^2}+\frac{j_\tau^0\nu\Omega_\tau^{\rm dc}\sin\theta_h}{(\Omega_\tau^{\rm dc})^2+\nu^2},\tag{41}$$

$$j_c^{\rm dc}\approx\frac{j_\tau^0\nu\Omega_\tau^{\rm dc}\cos\theta_h}{(\Omega_\tau^{\rm dc})^2+\nu^2},\tag{42}$$

are derived from Eqs. (33).

The linear conductivity regime is delineated by the satisfaction of the twin conditions $(\Omega_z^{\rm dc})^2\ll\nu^2$ and $(\Omega_\tau^{\rm dc})^2\ll\nu^2$. The corresponding axial and circumferential dc conductivities then emerge from Eqs. (18), (41), and (42) as follows:

$$\sigma_{zz}=\frac{j_z^{\rm dc}}{E_z^{\rm dc}}\approx\frac{e}{\hbar\nu}(j_z^0d_z+j_\tau^0d_\tau\sin^2\theta_h),\tag{43}$$

$$\sigma_{cz}=\frac{j_c^{\rm dc}}{E_z^{\rm dc}}\approx\frac{e}{\hbar\nu}j_\tau^0d_\tau\sin\theta_h\cos\theta_h.\tag{44}$$

The presence of the Planck constant in the denominators indicates the purely quantum nature of dc conduction in a CN. Furthermore, the circumferential conductivity σ_{cz} here is due to the curvature of the CN surface. Indeed, we observe that $\sigma_{cz}\to0$ and $\gamma\to\pi/2$ in the limit $R_h\to\infty$ (i.e., $\theta_h\to0$ because d_τ and d_z are constants in our model), in perfect accord with the results of the first-principles numerical simulations of Miyamoto, Louie, and Cohen.[12] This agreement adds to our confidence in the model used.

Figure 2 depicts the dependences of the CCA γ on the amplitude $E_z^{\rm dc}$ of the applied dc field as well as on the GCA θ_h. As $\Omega_z^{\rm dc}$ increases, γ decreases—which means that the circumferential current $j_c^{\rm dc}$ increases. On the other hand, Fig. 2 shows that $\gamma\approx\pi/2-\theta_h$ when $\Omega_z^{\rm dc}\ll\nu$ (the case simulated by Miyamoto, Louie, and Cohen[12]). This can also be established from Eqs. (39), (43), and (44) after assuming Eq. (24) to be hold. As far as $\theta_h\ll1$, one can conclude from the above that in CN's any effects resulting from the chirality will be extremely small in linear approximation with respect to $E_z^{\rm dc}$. As regards BC_2N nanotubes, chirality may give pronounced effects owing to the anisotropy inherent in their plane crystalline structure.

Another mechanism of conductivity anisotropy, which can manifest itself both in carbon and BC_2N nanotubes, arises as the amplitude $E_z^{\rm dc}$ grows. This mechanism is different from that described by Miyamoto, Louie, and Cohen[12] and can be explained by interpreting the CN as a system of two interacting one-dimensional lattices. Thus, the flux $\mathcal{Z}$ describes the current on an axial lattice, while the flux $\mathcal{S}$ refers to a helical lattice. As is clear from Eqs. (41) and (42), the CCA γ depends on the amplitude $E_z^{\rm dc}$ in a strong dc field, bringing nonlinearity and anisotropy into play. The distinguished direction of the conductivity anisotropy in this mechanism is parallel to the direction of the applied dc field.

This new mechanism becomes significant in the regime $\Omega_z^{\rm dc}\geqslant\nu$. Now, the range $10^{10}\leqslant\nu\leqslant10^{12}$ Hz can be estimated from Refs. 36 and 37, with $\nu\simeq7\times10^{11}$ Hz at room temperature.[36] Taking $d_z\simeq1.42$ Å from Ref. 18 and assuming $\Omega_z^{\rm dc}\simeq\nu$, we find from Eq. (18) that the new mechanism is significant for $E_z^{\rm dc}\geqslant3\times10^4$ V/cm.

C. Time-averaged current with ac pumping

Let us now add a high-frequency pumping by altering the applied field to the following form:

$$\mathbf{E}=(E_z^{\rm dc}+E_z^{\rm ac}\cos\omega t)\mathbf{u}_z.$$

The ac pumping substantially changes the dc conductivity of the CN.[28] Analytical results follow on setting $\xi_{z2}^{\rm ac}=\xi_{\tau2}^{\rm ac}=0$ and $E_\tau^{\rm ac,dc}=E_z^{\rm ac,dc}\sin\theta_h$ in Eqs. (33), (37), and (38), our interest lying chiefly in nonlinear effects.

Expressions for time-averaged current components emerge after the right sides of Eq. (33) are averaged over the temporal period $2\pi/\omega$ of the applied ac field; thus,

$$\langle j_z\rangle=\langle\mathcal{Z}\rangle+\langle\mathcal{S}\rangle\sin\theta_h,\quad\langle j_c\rangle=\langle\mathcal{S}\rangle\cos\theta_h,\tag{45}$$

where the angular brackets denote time averaging. Omitting intermediate calculations, we get

$$\langle\mathcal{Z}\rangle\approx\nu j_z^0\int_0^\infty\exp(-\nu t')\sin(\Omega_z^{\rm dc}t')J_0(2\xi_{z1}^{\rm ac}\sin(\omega t'/2))dt',\tag{46}$$

$$\langle\mathcal{S}\rangle\approx\nu j_\tau^0\int_0^\infty\exp(-\nu t')\sin(\Omega_\tau^{\rm dc}t')J_0(2\xi_{\tau1}^{\rm ac}\sin(\omega t'/2))dt',\tag{47}$$

where $J_0(\cdot)$ is the cylindrical Bessel function of the order 0. Note that $\langle\mathcal{Z}\rangle,\langle j_z\rangle$ are even functions of θ_h while $\langle\mathcal{S}\rangle,\langle j_c\rangle$ are odd ones.

Suppose the direction of the externally applied electrostatic field is reversed: $\Omega_{z,\tau}^{\rm dc}\to-\Omega_{z,\tau}^{\rm dc}$. We observe from Eqs. (45)–(47) that the signs of both $\langle j_z\rangle$ and $\langle j_c\rangle$ then change, but γ, $|\langle j_z\rangle|$ and $|\langle j_c\rangle|$ remain unaltered.

Similarly, suppose that a structurally right-handed nanotube ($\theta_h>0$) is replaced by its mirror image or enantiomer: $\theta_h\to-\theta_h$. Again, as per Eqs. (45)–(47), the operation $\theta_h\to-\theta_h$ leads to $\langle j_z\rangle\to\langle j_z\rangle$ and $\langle j_c\rangle\to-\langle j_c\rangle$ which, in turn, imply that $\gamma\to-\gamma$.

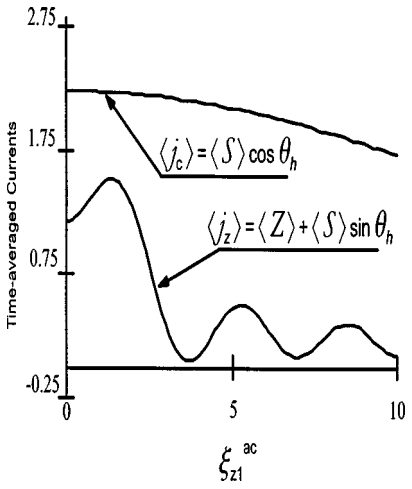

FIG. 3. Dimensionless time-averaged current components in a CN versus the ratio ξ_{z1}^{ac}. The plots were drawn with the following parameter values: $\nu=\omega/5$, $\Omega_z^{dc}=\omega+\nu$, and $\theta_h=4°$.

Figure 3 shows typical dependencies of $\langle j_z \rangle$ and $\langle j_c \rangle$ on the dimensionless amplitude ξ_{z1}^{ac} of the ac pump. The time-averaged circumferential current $\langle j_c \rangle$ varies slowly with respect to ξ_{z1}^{ac}, but the time-averaged axial current $\langle j_z \rangle$ presents a strongly undulating profile. The result is that the GCA varies with the ac pumping amplitude also in a complicated fashion, as depicted in Fig. 4.

In particular, there are values of E_z^{ac} at which $\gamma = \tan^{-1}(\langle j_z \rangle / \langle j_c \rangle) \simeq 0$, so that the circumferential current dominates and the net time-averaged current is almost perpendicular to the applied electrostatic field. Suppose, as in Sec. IV B that $\nu \simeq 7\times10^{11}$ Hz and $d_z \simeq 1.42$ Å; and that $\Omega_z^{dc} \simeq 4.2\times10^{12}$ Hz. Let the ac pumping operate at the angular frequency $\omega \simeq 3.5\times10^{12}$ rad/s. From Fig. 4, we see that $\gamma \approx 0$ when $\xi_{z1}^{ac} \simeq 4$. Thus, when $E_z^{ac} \simeq 6.5\times10^5$ V/cm and $E_z^{dc} \simeq 1.94\times10^5$ V/cm, the net time-averaged current is almost purely circumferential even though the total applied electric field is purely axial. The physical explanation for this effect is as follows: the axial current in the CN consists of two components—one caused by electron motion along the base helix, the other by electron motion along the tubular axis from turn to turn. The ac pumping changes their ratio, sometimes resulting in almost totally destructive interference.

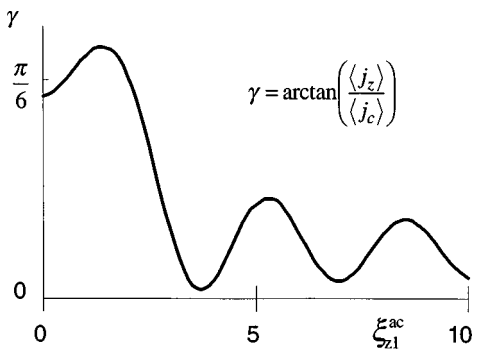

FIG. 4. Current chiral angle γ as a function of the ratio ξ_{z1}^{ac}, when $\nu=\omega/5$, $\Omega_z^{dc}=\omega+\nu$, and $\theta_h=4°$.

V. EFFECTIVE JUMP CONDITIONS ACROSS THE NANOTUBE SURFACE

A. Exposure to ac field alone

Let us now use the results of Sec. IV A to study wave propagation phenomena. We consider an infinitely long nanotube in free space (i.e., vacuum) exposed to a monochromatic electro-magnetic field. The pitch and the radius of the nanotube are assumed to be much smaller than the wavelength of the electromagnetic field, and $\mathbf{E}^{dc}=\mathbf{0}$. Furthermore, the amplitudes of both the applied ac electric field and the surface density of the induced current are weak so that linearization of the right sides of Eqs. (37) and (38) with respect to $\xi_{z1,2}^{ac}$ and $\xi_{\tau1,2}^{ac}$ is possible. Phasor notation is very suitable for the developments in this section; thus, the electric field, the magnetic field, and the electric surface current density are, respectively, stated as follows:

$$\mathbf{E}_{ac}(t)=\mathrm{Re}\{\mathbf{E}\ \exp(-i\omega t)\}=\mathbf{E}_{ac}^{(1)}\ \cos(\omega t)+\mathbf{E}_{ac}^{(2)}\ \sin(\omega t),$$
$$\mathbf{H}_{ac}(t)=\mathrm{Re}\{\mathbf{H}\ \exp(-i\omega t)\}, \tag{48}$$
$$\mathbf{J}_{ac}(t)=\mathrm{Re}\{\mathbf{J}\ \exp(-i\omega t)\}.$$

We assume that the density of electric surface current is similarly distributed throughout the nanotube surface, because both the pitch p_h and the radius R_h are small and the surface may be considered as a continuous current sheet. Ohm's law on the nanotube surface may then be stated as

$$\mathbf{J}(\mathbf{r})=\hat{\sigma}^{ac}(\mathbf{r})\cdot\mathbf{E}(\mathbf{r});\quad \rho=R_h, \tag{49}$$

where

$$\hat{\sigma}^{ac}(\mathbf{r})=\sigma_z\mathbf{u}_z\mathbf{u}_z+\sigma_\tau\mathbf{u}_\tau(\mathbf{r})\mathbf{u}_\tau(\mathbf{r}) \tag{50}$$

is the ac surface conductivity tensor with components

$$\sigma_z=i\,\frac{ed_zj_z^0}{\hbar\omega},\quad \sigma_\tau=i\,\frac{ed_\tau j_\tau^0}{\hbar\omega}. \tag{51}$$

The two components of $\hat{\sigma}^{ac}(\mathbf{r})$ are evaluated by retaining only the first terms in the Maclaurin expansion of $\sin\{\cdot\}$ on the right sides of Eqs. (37) and (38), and then putting $\Omega_z^{dc}=\Omega_\tau^{dc}=0$ therein. Clearly, $\hat{\sigma}^{ac}(\mathbf{r})$ is purely reactive and does not give rise to energy dissipation. Furthermore, it denotes *surface* conduction (and not *volumetric* conduction) because it is constituted by the two-dimensional nature of electron transport in a nanotube. Finally, the various unit vectors on the nanotube surface are no longer specified on the base helix, but everywhere on a continuous cylindrical surface of radius $\rho=R_h$.

As Eq. (49) holds on the nanotube surface, it can be used to determine the jumps in the electric and the magnetic fields across the surface. Let all space be divided by the infinitely long nanotube into two regions: region I ($\rho<R_h$) and region II ($\rho>R_h$). Since no magnetic surface current density is excited on the surface, the usual jump condition

$$\mathbf{u}_n(\mathbf{r})\times[\mathbf{E}^{I}(\mathbf{r})-\mathbf{E}^{II}(\mathbf{r})]=\mathbf{0};\quad \rho=R_h \tag{52}$$

holds for the electric field. However, the electric surface current density creates a discontinuity in the tangential component of the magnetic field; thus,

$$\frac{c}{4\pi}\,\mathbf{u}_n(\mathbf{r})\times[\mathbf{H}^{\mathrm{I}}(\mathbf{r})-\mathbf{H}^{\mathrm{II}}(\mathbf{r})]=\mathbf{J}(\mathbf{r});\quad \rho=R_h. \tag{53}$$

Hence, in view of Eq. (49), the boundary conditions on the surface $\rho=R_h$ may be stated as

$$\begin{aligned}\frac{c}{4\pi}\,&\mathbf{u}_n(\mathbf{r})\times[\mathbf{H}^{\mathrm{I}}(\mathbf{r})-\mathbf{H}^{\mathrm{II}}(\mathbf{r})]\\ &=\hat{\sigma}^{\mathrm{ac}}(\mathbf{r})\cdot\mathbf{E}^{\mathrm{II}}(\mathbf{r})\\ &=-\hat{\sigma}^{\mathrm{ac}}(\mathbf{r})\cdot\{\mathbf{u}_n(\mathbf{r})\times[\mathbf{u}_n(\mathbf{r})\times\mathbf{E}^{\mathrm{II}}(\mathbf{r})]\};\quad \rho=R_h.\end{aligned} \tag{54}$$

The second equality follows from the fact that $\mathbf{u}_n(\mathbf{r})\cdot\hat{\sigma}^{\mathrm{ac}}=\hat{\sigma}^{\mathrm{ac}}\cdot\mathbf{u}_n(\mathbf{r})=\mathbf{0}$.

Further manipulations allow reduction of Eq. (54) to the conventional form of impedance boundary conditions. Thus,

$$\begin{aligned}\{\mathbf{u}_n(\mathbf{r})\times[\mathbf{u}_n(\mathbf{r})\times\mathbf{E}^{\mathrm{II}}(\mathbf{r})]\}&\\ =i\hat{\zeta}^{\mathrm{ac}}\cdot[\mathbf{u}_n(\mathbf{r})\times[\mathbf{H}^{\mathrm{I}}(\mathbf{r})-\mathbf{H}^{\mathrm{II}}(\mathbf{r})]];&\quad \rho=R_h,\end{aligned} \tag{55}$$

with the ac surface impedance tensor given by

$$\hat{\zeta}^{\mathrm{ac}}=\frac{ic}{4\pi\sigma_\tau\sigma_z\cos^2\theta_h}\,(\sigma_\tau\mathbf{u}_b\mathbf{u}_b+\sigma_z\mathbf{u}_\phi\mathbf{u}_\phi). \tag{56}$$

Both components of $\hat{\zeta}^{\mathrm{ac}}$ are real-valued quantities. As neither component depends on the spatial characteristics of the illuminating wave, the boundary condition (55) is local but anisotropic.

Impedance boundary conditions are widely used in the theory of helical slow-wave systems and helical antennas.[38–40] In particular, Eq. (55) allows us to connect helically conducting cylinders (HEC's) with nanotubes. As the surface conductivity of a HEC is infinite along the base helix but null in the binormal direction, all foregoing equations for a nanotube are applicable in the limits $|\sigma_\tau|\to\infty$ and $\sigma_z\to 0$.

The impedance boundary condition for achiral CN's (Ref. 31) also has the form of Eq. (55) with the transformed ac surface impedance tensor. First, the replacement $N\sin\theta_h\to d_z/d_\tau$ has to be made in the foregoing equations; then, the limit $\theta_h\to 0$ has to be taken. Finally, after applying conditions (24), one can obtain

$$\hat{\zeta}^{\mathrm{ac}}_{\mathrm{achi}}\simeq\frac{ic}{4\pi\sigma^{\mathrm{ac}}_{\mathrm{achi}}}\,(\mathbf{u}_z\mathbf{u}_z+\mathbf{u}_\phi\mathbf{u}_\phi) \tag{57}$$

of an achiral nanotube emerges as an isotropic entity, with

$$\sigma^{\mathrm{ac}}_{\mathrm{achi}}=in_0\,\frac{(ed_z)^2\Delta_z}{\hbar^2\omega}\,\frac{I_1(\Delta_z/k_BT)}{I_0(\Delta_z/k_BT)}. \tag{58}$$

Parenthetically, we have also calculated $\sigma^{\mathrm{ac}}_{\mathrm{achi}}$ based on a model that properly incorporates the actual hexagonal crystalline structure of graphite. Instead of Eq. (23), we used a Hamiltonian suggested by Wallace.[41] Although calculations with the latter Hamiltonian became much more complicated, the results are in good agreement with Eq. (58). This fact substantiates the applicability of our phenomenological model of a nanotube described in Sec. 2. A detailed comparative study will be provided in a separate paper.

B. Simultaneous exposure to ac and dc fields

Let us now expose the nanotube simultaneously to a dc electric field $\mathbf{E}_{\mathrm{dc}}=E^{\mathrm{dc}}_z\mathbf{u}_z$. Equations (37)–(39) are applicable with $E^{\mathrm{dc}}_\tau=E^{\mathrm{dc}}_z\sin\theta_h$ and $\Omega^{\mathrm{dc}}_\tau=\Omega^{\mathrm{dc}}_z(d_\tau/d_z)\sin\theta_h$. Assuming that the amplitude of the high-frequency electric field is small, we linearize the right sides of Eqs. (37) and (38) with respect to $\xi^{\mathrm{ac}}_{z1,2}$ and $\xi^{\mathrm{ac}}_{\tau1,2}$, and evaluate the time-dependent parts of the currents j_z and j_c in Eq. (33) analytically. As a result,

$$\begin{aligned}\sigma_z&=-j^0_z\nu\,\frac{ed_z}{\hbar\omega}\,[C_z-i(A_z-B_z)],\\ \sigma_\tau&=-j^0_\tau\nu\,\frac{ed_\tau}{\hbar\omega}\,[C_\tau-i(A_\tau-B_\tau)],\end{aligned} \tag{59}$$

where

$$\begin{aligned}A_{z,\tau}&=\int_0^\infty e^{-\nu t'}\cos(\Omega^{\mathrm{dc}}_{z,\tau}t')\,dt'=\frac{\nu}{(\Omega^{\mathrm{dc}}_{z,\tau})^2+\nu^2},\\ B_{z,\tau}&=\int_0^\infty e^{-\nu t'}\cos(\Omega^{\mathrm{dc}}_{z,\tau}t')\cos(\omega t')\,dt'\\ &=\frac{\nu}{2}\left[\frac{1}{(\Omega^{\mathrm{dc}}_{z,\tau}-\omega)^2+\nu^2}+\frac{1}{(\Omega^{\mathrm{dc}}_{z,\tau}+\omega)^2+\nu^2}\right],\\ C_{z,\tau}&=-\int_0^\infty e^{-\nu t'}\cos(\Omega^{\mathrm{dc}}_{z,\tau}t')\sin(\omega t')\,dt'\\ &=-\frac{1}{2}\left[\frac{\omega-\Omega^{\mathrm{dc}}_{z,\tau}}{(\Omega^{\mathrm{dc}}_{z,\tau}-\omega)^2+\nu^2}+\frac{\omega+\Omega^{\mathrm{dc}}_{z,\tau}}{(\Omega^{\mathrm{dc}}_{z,\tau}+\omega)^2+\nu^2}\right].\end{aligned} \tag{60}$$

As $\Omega^{\mathrm{dc}}_{z,\tau}\to 0$ (i.e., for a weak dc field), we get $A_{z,\tau}\to\nu^{-1}$, $B_{z,\tau}\to\nu/(\nu^2+\omega^2)$ and $C_{z,\tau}\to-\omega/(\nu^2+\omega^2)$. For small ν, only the terms containing $A_{z,\tau}$ are significant, so that Eqs. (59) simplify to Eqs. (51).

VI. SURFACE WAVE PROPAGATION

A. Dispersion equation

Being very long, a nanotube can guide electromagnetic waves. Let us consider therefore guided wave propagation in an isolated nanotube, the surrounding medium being free space (i.e., vacuum).

The electromagnetic field phasors associated with a cylindrical eigenwave are written in terms of electric and magnetic Hertz vectors, $\mathbf{\Pi}_\epsilon$ and $\mathbf{\Pi}_\mu$, as

$$\begin{aligned}\mathbf{E}&=\nabla(\nabla\cdot\mathbf{\Pi}_\epsilon)+k^2\mathbf{\Pi}_\epsilon+ik\nabla\times\mathbf{\Pi}_\mu,\\ \mathbf{H}&=-ik\nabla\times\mathbf{\Pi}_\epsilon+\nabla(\nabla\cdot\mathbf{\Pi}_\mu)+k^2\mathbf{\Pi}_\mu,\end{aligned} \tag{61}$$

where $k=\omega/c$ is the wave number in free space, $\mathbf{\Pi}_{\epsilon,\mu}=\Pi_{\epsilon,\mu}\mathbf{u}_z e^{ihz}$ and h is the guide wave number. Assuming polar symmetry (i.e., $\partial/\partial\phi\equiv 0$), we state the scalar Hertz vectors as[38]

$$\Pi_\epsilon = A\begin{Bmatrix} I_0(\kappa\rho)K_0(\kappa R_h) \\ I_0(\kappa R_h)K_0(\kappa\rho)\end{Bmatrix}, \quad \Pi_\mu = B\begin{Bmatrix} I_0(\kappa\rho)K_0'(\kappa R_h) \\ I_0'(\kappa R_h)K_0(\kappa\rho)\end{Bmatrix}. \tag{62}$$

Here, $\kappa = +\sqrt{h^2 - k^2}$ is the transverse wave number; A and B are unknown coefficients; $I_0(\cdot)$ and $K_0(\cdot)$ are the modified Bessel functions of order 0; while the prime indicates differentiation with respect to the argument. The upper rows on the right sides of Eqs. (62) apply in region I ($\rho < R_h$), and the lower rows in region II ($\rho > R_h$).

The electromagnetic field components needed to solve the guided wave problem are obtained from the scalar Hertz vectors as

$$E_\varphi = -ik\,\frac{\partial \Pi_\mu}{\partial \rho}\,e^{ihz}, \quad E_z = -\kappa^2 \Pi_\epsilon e^{ihz}, \tag{63}$$

and

$$H_\varphi = ik\,\frac{\partial \Pi_\epsilon}{\partial \rho}\,e^{ihz}, \quad H_z = -\kappa^2 \Pi_\mu e^{ihz}. \tag{64}$$

The jump condition (52) is satisfied identically. In order to satisfy the boundary condition (55), we first use Eqs. (62) and (64), as well as the Wronskian equality $I_0'(y)K_0(y) - I_0(y)K_0'(y) = 1/y$, to get

$$\lim_{\rho \to R_h} (H_z^{\mathrm{I}} - H_z^{\mathrm{II}}) = \frac{\kappa B}{R_h}\,e^{ihz}, \quad \lim_{\rho \to R_h} (H_\varphi^{\mathrm{I}} - H_\varphi^{\mathrm{II}}) = i\,\frac{kA}{R_h}\,e^{ihz}. \tag{65}$$

Then, substituting expressions (63) and (65) in Eq. (55), we obtain two algebraic equations, viz.,

$$-ik\zeta_{12}A + [k\kappa R_h I_1(\kappa R_h)K_1(\kappa R_h) + \kappa\zeta_{11}]B = 0,$$

$$[\kappa^2 R_h I_0(\kappa R_h)K_0(\kappa R_h) - k\zeta_{22}]A - i\kappa\zeta_{12}B = 0. \tag{66}$$

These equations have a nontrivial solution for A and B for those values of κ (or h) that satisfy the dispersion equation,

$$\left(kI_1(\kappa R_h)K_1(\kappa R_h) + \frac{\zeta_{11}}{R_h}\right)\left(\kappa^2 I_0(\kappa R_h)K_0(\kappa R_h) - \frac{k\zeta_{22}}{R_h}\right) + \zeta_{12}^2\,\frac{k}{R_h^2} = 0. \tag{67}$$

Equation (67) is general and can be used for any model of nanotube conductivity, the choice of model affecting $\hat{\zeta}^{\mathrm{ac}}$ only. In the following, we employ Eq. (56).

After using the relation $\zeta_{12} = \zeta_{22}\tan\theta_h$, the dispersion equation (67) can be transformed into a form analogous to that for HEC's;[38] thus,

$$\left(\frac{\kappa}{k}\right)^2 = \frac{1}{Q(\kappa)}, \tag{68}$$

where the quality factor

$$Q(\kappa) = \frac{\zeta_{11}}{\zeta_{22}}\,\frac{I_0(\kappa R_h)K_0(\kappa R_h)}{I_1(\kappa R_h)K_1(\kappa R_h) + (\zeta_{11} - \zeta_{22}\tan^2\theta_h)/k R_h} \times\left[1 + \frac{kR_h}{\zeta_{11}}\,I_1(\kappa R_h)K_1(\kappa R_h)\right]. \tag{69}$$

Equation (68) is a transcendental equation for κ. Recalling that $\hat{\zeta}^{\mathrm{ac}}$ is proportional to ω, we observe that the right side of Eq. (69) does not depend upon k.

On applying the limits $|\sigma_\tau| \to \infty$ and $\sigma_z \to 0$, we see that $\zeta_{11} \to \infty$ and $\zeta_{11} \to \zeta_{22}\tan^2\theta_h$. The quality factor then simplifies to

$$Q(\kappa) = \tan^2\theta_h\,\frac{I_0(\kappa R_h)K_0(\kappa R_h)}{I_1(\kappa R_h)K_1(\kappa R_h)}, \tag{70}$$

which is the same as for a HEC.[38]

B. Dispersion characteristics analysis

Returning to Eq. (69), let us introduce the dimensionless variables $u = \kappa R_h \tan\theta_h$ and $q = kR_h \tan\theta_h$ and define the parameter $\eta = \sqrt{u^2 + q^2}$. Then, parametric solutions of the dispersion equation (68) in terms of u may be obtained as

$$\eta = \pm\sqrt{1 + Q(uR_h^{-1}\cot\theta_h)}, \tag{71}$$

$$q = x\sqrt{Q(xR_h^{-1}\cot\theta_h)}. \tag{72}$$

The slow-wave coefficient $\beta = k/h$ is expressed as

$$\beta = \sqrt{\frac{Q(uR_h^{-1}\cot\theta_h)}{1 + Q(uR_h^{-1}\cot\theta_h)}}. \tag{73}$$

For a qualitative analysis of the dispersion equation (67), we set $\kappa R_h \gg 1$, which implies field concentration near the CN. Then, $I_1(\kappa R_h)K_1(\kappa R_h) \sim I_0(\kappa R_h)K_0(\kappa R_h) \sim (2\kappa R_h)^{-1}$, and Eq. (67) simplifies as follows:

$$(\kappa - 2\zeta_{22}k)(k + 2\zeta_{11}\kappa) + 4\zeta_{22}^2 k\kappa\tan^2\theta_h = 0. \tag{74}$$

This quadratic equation has the two solutions

$$\kappa = \frac{k}{4\zeta_{11}}\,[-b \pm \sqrt{b^2 + 16\zeta_{11}\zeta_{22}}], \tag{75}$$

where $b = 1 + 4\zeta_{22}(\zeta_{22}\tan^2\theta_h - \zeta_{11}) = 1 - 4(\sigma_z\sigma_\tau\cos^2\theta_h)^{-1}$. Only the positive solutions of Eq. (74) are physical, as they lead to the satisfaction of the radiation conditions as $\rho \to \infty$. When $\zeta_{11} > 0$, the proper solution,

$$\kappa = \frac{k}{4\zeta_{11}}\,[-b + \sqrt{b^2 + 16\zeta_{11}\zeta_{22}}], \tag{76}$$

characterizes surface wave propagation in the nanotube.

Let us restrict ourselves to the case of CN's, assuming condition (24) to be valid. It means that $\zeta_{11} = \zeta_{22}$. Then, the ac surface impedance tensor can be transformed into the frequency-independent scalar

$$\tilde{\zeta} = \frac{\zeta_{11}}{kR_h} \simeq \left(\frac{\hbar c}{e d_z}\right)^2 \frac{I_0(\Delta_z/k_B T)}{4\pi n_0 R_h \Delta_z I_1(\Delta_z/k_B T)}. \tag{77}$$

By setting $d_z \simeq 1.42$ Å, $\Delta_z \simeq 2$ eV,[20] $n_0 \simeq 2.27 \times 10^{14}$ cm^{-2},[7] $R_h \simeq 20$ Å, and $T \simeq 300$ K, we get the estimate $\tilde{\zeta} \simeq 1.16 \times 10^4$.

Figure 5 shows computed values of the slow-wave coefficient $\beta = k/h$ for an achiral CN ($\theta_h = 0$) for different $\tilde{\zeta}$, when $\tilde{\zeta}_{11} = \tilde{\zeta}_{22}$. Surface waves with ϕ-independent fields do

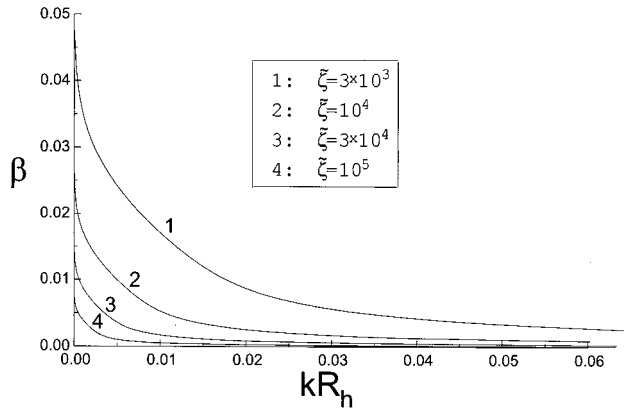

FIG. 5. Slow-wave coefficient $\beta=k/h$ for an achiral nanotube ($\theta_h=0$) for different $\tilde{\zeta}$, when $\tilde{\zeta}_{11}=\tilde{\zeta}_{22}$.

not possess any critical frequency, and $\beta\to1$ as $kR_h\to0$. The electromagnetic field is concentrated near the CN surface $\rho=R_h$ (see Fig. 6), because $\tilde{\zeta}$ has large values in nanotubes.

The dispersion equation for the surface waves being considered depends slightly on the angle θ_h. The dependence is slight, because we linearized the results of the previous sections in this one. Nonlinear electromagnetic phenomena will be considered in a separate paper.

The frequency range for validity of the presented CN conductivity model can be deduced from the inequality

$$\hbar\nu<\hbar\omega\ll2\Delta_z\leqslant2\Delta_g, \tag{78}$$

where Δ_g is the width of the forbidden band.[42] Using $\Delta_z\simeq2$ eV and $\nu\simeq5\times10^{11}$ Hz, we see that the estimated range 10^{11} Hz$<\omega/2\pi<2\times10^{14}$ Hz lies in the infrared portion of the spectrum, which means that a CN can serve as a nanowaveguide at infrared frequencies. For $R_h\simeq2$ nm then, we have $2\times10^{-5}<kR_h<8\times10^{-3}$.

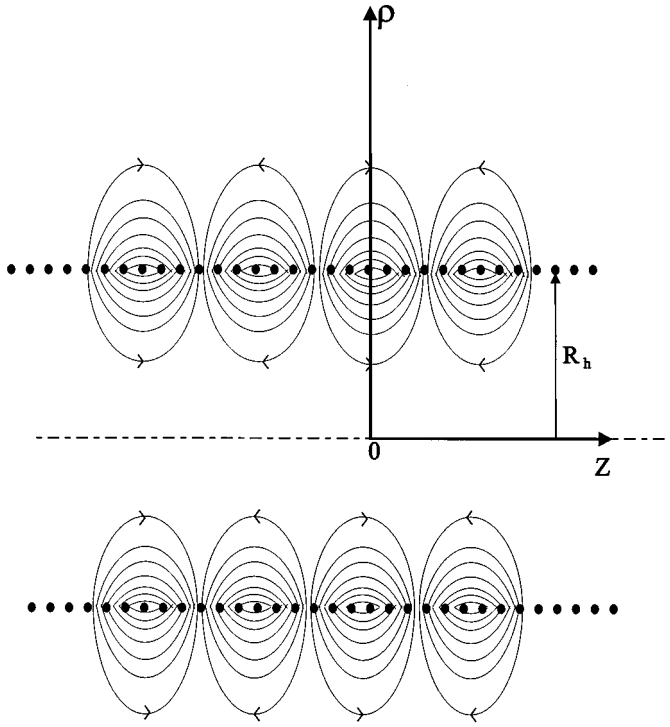

FIG. 6. Electric field structure for the surface wave in an achiral nanotube ($\theta_h=0$).

Let us also estimate the lower limit of β for which the presented CN conductivity model holds. In Sec. IV, we effectively neglected all spatial derivatives in deriving Eq. (34). This neglect is valid if $(v_zh)^2\ll\omega^2$, where $v_z\sim\Delta_zd_z/\hbar$ is the maximum electron velocity. Then we have $\beta>3v_z/c\simeq0.5\times10^{-2}$. If β is smaller, the dependence of $\mathbf{u}_\tau(s)$ on s cannot be ignored and spatially inhomogeneous terms on the right side of Eq. (25) must be taken into account, which cause $\tilde{\zeta}$ to depend on h although Eq. (69) still holds for the quality factor.

VII. NANOWAVEGUIDE IMMERSED IN dc FIELD: INSTABILITIES OF WAVES

A. Achiral nanowaveguide

Consider a nanowaveguide immersed in an axial dc electric field $\mathbf{E}_{\rm dc}=E_z^{\rm dc}\mathbf{u}_z$. The dispersion equation for surface wave propagation (with ϕ-independent fields) has the same form as Eq. (67). However, σ_τ and σ_z now have to be determined from Eqs. (59).

Let us commence with *achiral* nanotubes: $\theta_h\to0$. The dispersion equation then turns out to be as follows:

$$\left(\frac{\kappa}{k}\right)^2I_0(\kappa R_h)K_0(\kappa R_h)=\frac{\zeta_{22}}{kR_h}. \tag{79}$$

Assuming $|\kappa|R_h>1$, we find

$$\kappa=\kappa'+i\kappa''\cong2k\zeta_{22}=\frac{kc}{2\pi\sigma_z} \tag{80}$$

as an approximate solution, with σ_z given by Eq. (59).

The existence condition for surface wave propagation is $\kappa'>0$, or $A_z-B_z>0$ equivalently. Using Eqs. (60), we have the result

$$\omega^2+\nu^2>3(\Omega_z^{\rm dc})^2. \tag{81}$$

An important deduction immediately follows: as distinct from the case illustrated at Fig. 5, a sufficiently strong dc field may give rise to a critical frequency such that surface waves with polar symmetry cannot propagate at frequencies lower than the critical frequency. The minimum dc field amplitude is found from the condition $\Omega_z^{\rm dc}>\nu/\sqrt{3}$.

The instability condition is $\kappa''>0$, i.e., $C_z<0$. Again, using Eqs. (60), we have the equivalent expression

$$\omega^2+\nu^2<(\Omega_z^{\rm dc})^2. \tag{82}$$

On comparing the inequalities (81) and (82), we conclude that surface wave propagation in an achiral nanotube is stable.

However, this statement does not imply that ac field instability caused by amplification at the expense of the dc field is impossible in an achiral nanotube. When

$$\Omega_z^{\rm dc}>\sqrt{\omega^2+\nu^2}, \tag{83}$$

the solution given by Eq. (80) along with Eqs. (62), (63), and (64) describes a leaky surface wave with $\kappa'<0$ and $\kappa''<0$.

The guide wave number $h=h'+ih''$ is complex-valued with $h'h''=\kappa'\kappa''$. If $h'>0$, then $h''>0$; i.e., the fields delineated by Eqs. (63) and (64) intensify with increasing ρ but decrease along the z axis, as it should be for leaky waves.[43]

The energy flux Σ_ρ transferred to a surface wave at the surface $\rho=R_h$ is given by

$$\Sigma_\rho=-\frac{c}{8\pi}\lim_{\delta\to 0}[\mathbf{u}_n\cdot\mathrm{Re}\{[\mathbf{E}\times\mathbf{H}^*]|_{\rho=R_h+\delta} -[\mathbf{E}\times\mathbf{H}^*]|_{\rho=R_h-\delta}\}]=-\frac{kc}{4\pi|\kappa|^2}\kappa''|E_z|^2|_{\rho=R_h}, \tag{84}$$

where the asterisk indicates the conjugate transpose. If $\kappa''<0$, Eq. (84) yields $\Sigma_\rho>0$, which means that the surface wave is amplified by the applied dc field, and the added energy is leaked into outer space. Hence, a convective instability of the high-frequency field develops in a nanotube, if the inequality (83) holds.

B. Chiral nanowaveguide

Let us now elucidate another type of instability, which is peculiar to nanotubes. For a simple analysis, let us assume that

$$\nu\ll\omega, \quad \nu\ll|\Omega^{\mathrm{dc}}_{z,\tau}-\omega|. \tag{85}$$

Equations (59) then yield

$$\sigma_z\simeq-\frac{ij^0_z\nu e d_z/\hbar}{\omega^2-(\Omega^{\mathrm{dc}}_z)^2}, \quad \sigma_\tau\simeq-\frac{ij^0_\tau\nu e d_\tau/\hbar}{\omega^2-(\Omega^{\mathrm{dc}}_\tau)^2}, \tag{86}$$

for use in the dispersion equation (68). Furthermore, when β is large, Eq. (68) simplifies to Eq. (74).

The physical value of κ is then given by Eq. (75) with the upper sign. Although $\mathrm{Re}(\kappa)>0$, in contrast to the developments in Sec. 6, the guide wave number $h=\sqrt{k^2+\kappa^2}$ may be a complex-valued quantity with $\mathrm{Re}(h)>0$ and $\mathrm{Im}(h)<0$. The surface wave then becomes unstable when the following conditions also hold simultaneously:

$$\sigma_z\sigma_\tau\cos^2\theta_h>4, \quad \sigma^2_\tau\cot^2\theta_h>-4. \tag{87}$$

Equations (86) permit us to rewrite these two inequalities compactly as

$$\frac{\omega}{N}\sqrt{\frac{1+\alpha N^2}{1+\alpha}}<\Omega^{\mathrm{dc}}_\tau<\omega, \tag{88}$$

where $\alpha=j^0_z/(j^0_\tau N\sin\theta_h)$.

Clearly, the inequality (88) shows that surface wave propagation in a CN is unstable when E^{dc}_z lies in a certain range. This range narrows as α increases; and the range shrinks to a point as $\alpha\to\infty$ (i.e., $j^0_z\to 0$). Consequently, the instability is suppressed if electron motion is inhibited along the tubular axis. The instability disappears when $\theta_h\to 0$, when the range of appropriate values of E^{dc}_z becomes infinite. Parenthetically, when correlation (24) holds true, condition (88) reduces to $\omega/\sqrt{2}<\Omega^{\mathrm{dc}}_\tau<\omega$.

As the instability at any location does not increase with the passage of time, it is a convective instability. It corresponds to the amplification regime of an input signal, the dc field providing the energy needed for amplification.

The inequality (88) holds if we have $\nu\simeq 10^{10}$ Hz, $\omega\simeq 10^{11}$ rad/s, $d_z=d_\tau=1.42$ Å, $\Delta_z=\Delta_\tau$, and $\sin\theta_h\sim 0.1$. Taking $\Omega^{\mathrm{dc}}_z\simeq 0.75\times 10^{12}$ Hz, we ensure that the conditions (85) are fulfilled. We then need $E^{\mathrm{dc}}_z\simeq 3\times 10^4$ V/cm to obtain the instability. But this instability is likely to be much harder to observe experimentally than the one considered in Sec. VII A. The value of ν we use is rather small, although it is accessible at low temperature.[36] Any increase in ν leads to a sharp growth of the dc field amplitude needed. Yet this instability provides an unusual example of how chirality can crucially affect the physical responses of nanotubes.

VIII. CONCLUDING REMARKS

The principal result of this work comprises three equations: (33), (37), and (38). They describe the electric current in a nanotube exposed simultaneously to constant and high-frequency fields. Several physical effects were identified using these equations.

The dependence of the CCA on the ac electric field amplitude was elucidated for the electron transport problem. At certain amplitudes of the ac electric field, the axial component of the time-varying current was shown to vanish, and only the circumferential component remained. This effect can possibly be observed as a sharp increase in the dc resistivity of a nanotube at specific amplitudes of the ac field. Another way to observe this effect may be to measure the variation of the magnetic field direction as the amplitude of the ac electric field changes. The identified effect may be useful for mapping nanotube geometry.

We also investigated surface wave propagation in nanotubes, proposing for the first time the concept of nanotubes as nanowaveguides. The surface wave propagates along the nanotube surface if the dc electric field is absent. Otherwise, leaky wave propagation is possible. If the nanotube is exposed to a dc electric field of appropriate magnitude, the surface wave can exhibit an instability with respect to small perturbations of electromagnetic field. This suggests the possibility of ac signal amplification, with energy supplied by the dc field. Whereas nanotubes may serve as transmission lines at infrared frequencies, the instability may be applied for amplification in nanoelectronics.

The electron transport effects predicted in Sec. IV can also be observed in planar two-dimensional superlattices, with the nonorthogonality of axes playing a role akin to that of chirality. It can be realized by using one-dimensional superlattices irradiated by strong ultrasonic standing waves.[25] Thus additional modulation will simulate some features of a nanotube. However, nanotubes display different electromagnetic characteristics in comparison with the quantum superlattices,[25] because they are hollow and possess chiral symmetry. Consequently, surface conduction takes place in single-wall nanotubes, but volumetric conduction occurs in superlattices. Electromagnetic effects analogous to those described in Secs. VI and VII will take place only in the so-called surface superlattices of different types.[46] Our technique may be applied for theoretical analysis of chiral nanostructures.[47,48]

We must emphasize again that our model is phenomeno-

logical and, accordingly, approximate. For example, it does not take the real hexagonal graphite structure of CN's into exact account. For adaptation to real CN's and BC_2N nanotubes, the phenomenological parameters Δ_τ, Δ_z, d_τ, and d_z will have to be determined either experimentally or even through the first-principles numerical simulations.

The hexagonal graphite structure can also be exactly studied with our approach, by replacing the semiclassical Hamiltonian (23) by more accurate expressions.[44] On effecting that replacement, expressions for the equilibrium distribution function $F(\mathbf{p})$ and the electron velocity $\mathbf{v}$ become more complicated than Eqs. (28) and (30), respectively. Therefore, the integrals in Eqs. (31), (32), and (35) cannot be evaluated analytically, and must be subjected to numerical and/or asymptotic techniques. We shall consider this issue in a separate paper.

An important aspect of the presented work is the neglect of the dependence of $\mathbf{u}_\tau(s)$ on s, which allowed us to use the very simple expression (34) for the collision integral on the right side of Eq. (25). This simplification is untenable if β is small and/or ϕ-dependent fields must be considered. But a general solution, analogous to Eq. (35), can then not be found. Although linearization with respect to the ac field amplitudes reduces the analytical complexity somewhat, $\hat{\zeta}^{\mathrm{ac}}$ becomes an integral operator that describes nonlocal effects. Further research appears necessary.

Certain new theoretical problems can be identified. For instance, nanotubes are not infinitely long and edge diffraction needs to be investigated. That can be accomplished with a semi-infinite cylinder model, and the Wiener-Hopf technique[39] appears promising. Similarly, real CN's can display spatially inhomogeneous electromagnetic response properties. Indeed, connected CNs (Ref. 13) and CN heterojunctions[21] are known to exist, and may be conceived of as inhomogeneities in open waveguides. Scattering by these inhomogeneities will cause modal transformations and radiation losses.[45] Finally, only linear electromagnetic problems were discussed in Secs. VI and VII. Nonlinear high-frequency phenomena (such as harmonic generation and soliton propagation, etc.) will appear in a nanowaveguide with nonlinear surface impedance.

*Electronic address: maksim@inp.belpak.minsk.by
†Electronic address: axl4@psu.edu
‡Electronic addresses:
bom@mpipks-dresden.mpg.de; yevt@ire.kharkov.ua

[1] A. V. Eletskii and B. M. Smirnov, Usp. Fiz. Nauk **36** (2), 33 (1993) [Phys. Usp. **36** (3), 202 (1993)].
[2] A. V. Okotrub, D. A. Romanov, A. L. Chuvilin, Yu. V. Shevtsov, A. K. Gutakovskii, L. G. Bulusheva, and L. N. Mazalov, Phys. Low-Dimens. Semicond. Struct. **8/9**, 139 (1995).
[3] O. E. Omel'yanovskiĭ, V. I. Tsebro, O. I. Lebedev, A. N. Kiselev, V. I. Bondarenko, N. A. Kiselev, Z. Ja. Kosakovskaja, and L. A. Chernozatonskiĭ, Pis'ma Zh. Éksp. Teor. Fiz. **62**, 483 (1995) [JETP Lett. **62**, 503 (1995)].
[4] M. S. Dresselhaus, Nature (London) **358**, 195 (1992).
[5] N. M. Rodriguez, J. Mater. Res. **8**, 3233 (1993).
[6] P. J. Lin-Chung and A. K. Rajagopal, J. Phys.: Condens. Matter **6**, 3697 (1994).
[7] P. J. Lin-Chung and A. K. Rajagopal, Phys. Rev. B **49**, 8454 (1994).
[8] T. W. Ebbesen, Phys. Today **49** (6), 26 (1996).
[9] M. M. J. Treacy, T. W. Ebbesen, and J. M. Gibson, Nature (London) **381**, 678 (1996).
[10] T. W. Ebbesen, H. J. Lezec, H. Hiura, J. W. Bennett, H. F. Ghaemi, and T. Thio, Nature (London) **382**, 54 (1996).
[11] L. Lou, P. Nordlander, and R. E. Smalley, Phys. Rev. B **52**, 1429 (1995).
[12] Y. Miyamoto, S. G. Louie, and M. L. Cohen, Phys. Rev. Lett. **76**, 2121 (1996).
[13] R. Saito, G. Dresselhaus, and M. S. Dresselhaus, Phys. Rev. B **53**, 2044 (1996).
[14] L. X. Benedict, S. G. Louie, and M. L. Cohen, Phys. Rev. B **52**, 8541 (1995).
[15] A. Yu. Kasumov, I. I. Khodos, P. M. Ajayan, and C. Colliex, Europhys. Lett. **34**, 429 (1996).
[16] L. Langer, V. Bayot, E. Grivei, J.-P. Issi, J. P. Heremans, C. H. Olk, L. Stockman, C. Van Haesendonck, and Y. Bruynseraede, Phys. Rev. Lett. **76**, 479 (1996).
[17] O. V. Kibis, Fiz. Tverd. Tela **34**, 3511 (1992) [Sov. Phys. Solid State **34**, 1880 (1992)].
[18] D. A. Romanov and O. V. Kibis, Phys. Lett. A **178**, 335 (1993).
[19] D. A. Romanov, Pis'ma Zh. Èksp. Teor. Fiz. **55**, 703 (1992) [JETP Lett. **55**, 738 (1992)].
[20] O. V. Kibis and D. A. Romanov, Fiz. Tverd. Tela **37**, 127 (1995) [Phys. Solid State **37**, 69 (1995)].
[21] L. Chico, V. H. Crespi, L. X. Benedict, S. G. Louie, and M. L. Cohen, Phys. Rev. Lett. **76**, 971 (1996).
[22] O. Stephan, P. M. Ajayan, C. Colliex, Ph. Redlich, J. M. Lambert, P. Berneir, and P. Lefin, Science **266**, 1683 (1994).
[23] Z. Weng-Sieh, K. Cherrey, N. G. Chopra, X. Blase, Y. Miyamoto, A. Rubio, M. L. Cohen, S. G. Louie, A. Zettl, and R. Grousky, Phys. Rev. B **51**, 11 229 (1995).
[24] N. G. Chopra, R. J. Loyken, K. Cherrey, V. H. Crespi, M. L. Cohen, S. G. Louie, and A. Zettl, Science **269**, 966 (1995).
[25] F. G. Bass and A. A. Bulgakov, *Kinetic and Electrodynamic Phenomena in Classical and Quantum Semiconductor Superlattices* (Nova Science Publishers, New York, 1997).
[26] O. M. Yevtushenko, Phys. Rev. B **54**, 2578 (1996).
[27] O. M. Yevtushenko, Lith. Phys. J. **35**, 416 (1995).
[28] O. M. Yevtushenko, G. Ya. Slepyan, S. A. Maksimenko, A. Lakhtakia, and D. A. Romanov, Phys. Rev. Lett. **79**, 1102 (1997).
[29] G. Ya. Slepyan, S. A. Maksimenko, O. M. Yevtushenko, A. Lakhtakia, and A. V. Gusakov, in *Proceedings of Bianisotropics '97: International Conference Workshop on Electromagnetic Complex Media*, edited by W. S. Weiglhofer (University of Glasgow, Glasgow, 1997).
[30] R. Aris, *Vectors, Tensors, and the Basic Equations of Fluid Mechanics* (Prentice-Hall, Englewood Cliffs, NJ, 1962).
[31] M. S. Dresselhaus, G. Dresselhaus, and R. Saito, Solid State Commun. **84**, 201 (1992).
[32] In other words, we suppose that the temperature T is not very low so that $k_B T > N^{-2}\Delta_\tau$, which is quite reasonable because $N \gg 1$.
[33] I. M. Lifshits, M. Azbel, and M. I. Kaganov, *Electron Theory of Metals* (Consultants Bureau, New York, 1973).

[34] E. Zauderer, *Partial Differential Equations of Applied Mathematics* (Wiley, New York, 1989).
[35] M. Abramovitz and I. A. Stegun, *Handbook of Mathematical Functions* (Dover, New York, 1965); Eq. 9.6.34.
[36] R. A. Iishi, M. S. Dresselhaus, and G. Dresselhaus, Phys. Rev. B **48**, 11 385 (1993).
[37] O. Chauvet, L. Forro, W. Bacsa, D. Ugarte, B. Doudin, and W. A. de Heet, Phys. Rev. B **52**, R6963 (1995).
[38] L. Levin, *Theory of Waveguides* (Newnes-Butterworths, London, 1975).
[39] L. A. Weinstein, *The Theory of Diffraction and the Factorization Method* (Golem, New York, 1969).
[40] B. N. Basu, *Electromagnetic Theory and Applications in Beam-Wave Electronics* (World Scientific, Singapore, 1996).
[41] P. R. Wallace, Phys. Rev. **71**, 622 (1947).
[42] C. Kittel, *Introduction to Solid State Physics* (Wiley Eastern, New Delhi, 1974).
[43] L. B. Felsen and N. Marcuvitz, *Radiation and Scattering of Waves* (Prentice-Hall, Englewood Cliffs, NJ, 1973).
[44] M. F. Lin and K. W.-K. Shung, Phys. Rev. B **50**, 17 744 (1994); M. F. Lin and K. W.-K. Shung, *ibid.* **52**, 8423 (1995); W. Tian and S. Datta, *ibid.* **49**, 5097 (1994).
[45] L. A. Weinstein, *Open Resonators and Open Waveguides* (Golem, New York, 1969).
[46] P. D. Ye, D. Weiss, R. R. Gerhardts, M. Seeger, K. von Klitzing, K. Eberl, and H. Nickel, Phys. Rev. Lett. **74**, 3013 (1995); H. A. Carmona, A. K. Geim, A. Nogaret, P. C. Main, T. J. Foster, M. Henini, S. P. Beamont, and M. G. Blamire, *ibid.*, **74**, 3009 (1995); D. Weiss, K. von Klitzing, K. Ploog, and G. Weimann, Europhys. Lett. **8**, 179 (1989); R. R. Gerhardts, D. Weiss, and K. von Klitzing, Phys. Rev. Lett. **62**, 1173 (1989); R. W. Winkler, J. P. Kotthaus, and K. Ploog, *ibid.* **62**, 1177 (1989); A. Messica, A. Soibel, U. Meirav, A. Stern, H. Shtrikman, V. Umansky, and D. Mahalu, *ibid.* **78**, 705 (1997).
[47] K.-H. Ernst, C. F. McFadden, N. D. Spencer, M. Müller, U. Müller, and U. Ellerbeck, *Proceedings of Bianisotropics '97: International Conference Workshop on Electromagnetic Complex Media*, edited by W. S. Weiglhofer (University of Glasgow, Glasgow, 1997).
[48] H. Yang, N. Coombs, and G. A. Ozin, Nature (London) **386**, 692 (1997).